# Infrared spectra of nanometre granular zirconia

Hao Zhang†‖, Yulong Liu†, Ke Zhu†, Gueigu Siu‡, Yonghong Xiong§ and
Caoshui Xiong§

† Laboratory of Optical Physics, Institute of Physics, Chinese Academy of Sciences, PO Box
603, Beijing 100080, People's Republic of China
‡ Department of Physics and Materials Science, City University of Hong Kong, Tat Chee Avenue,
Kowloon, Hong Kong, People's Republic of China
§ Structure Research Laboratory, University of Science and Technology of China, Chinese
Academy of Sciences, Hefei, Anhui, 230026, People's Republic of China

**Abstract.**   High-quality Fourier-transform infrared reflectance spectra of nanometre $ZrO_2$ grains
with particle sizes ranging from 5 nm to 120 nm have been recorded at room temperature. The
results show that, even for very small grain sizes (5–10 nm), the samples retain the main features
of monoclinic symmetry, although the lowering of the crystal symmetry has led to the broadening
of the infrared bands. Two surface phonons have been identified. The processes of strain removal
above the 500 °C annealing temperature have been revealed by the appearance of two doublets
at around 435 $cm^{-1}$ and 375 $cm^{-1}$; at the same time the particle sizes increase rapidly. As the
particle size decreases, the doubly degenerate infrared-active modes, such as $2B_u$ at 511 $cm^{-1}$,
redshift while the non-degenerate modes, such as $A_u$ at 224 $cm^{-1}$, blueshift. This phenomenon is
tentatively explained in terms of the internal–external classification of the lattice vibrations.

It is well known that stabilized zirconia ($ZrO_2$) has many important applications such as
in high-temperature and high-pressure materials, fuel cells, and refractory materials. The
most common form of $ZrO_2$ is the $C_{2h}^5$ monoclinic structure with four molecules per unit cell
(m-$ZrO_2$) [1]. This can be transformed to a tetragonal structure possessing $D_{4h}^{15}$ symmetry
with two molecules per unit cell (t-$ZrO_2$) by either heating it to about 1425 K or doping it
with 12 mol% $Y_2O_3$ [2]. The possibility of using nanostructural oxides such as superfine
ceramics and nanometre semiconductors with different sizes and specific functions makes
their physical study interesting. In $ZrO_2$ nanograins, the quantum-size effect, the super-surface
effect, and the interaction of nanoclusters have been observed [3]. Earlier work [4] on Raman
and Fourier-transform infrared photoacoustic (FT-IR-PA) spectra of nanograin $ZrO_2$ found
some new spectral features, e.g. the appearance of surface phonons in Raman spectra of small
grains, and different behaviours of the absorption peaks below and above 1000 $cm^{-1}$ in FT-IR-
PA spectra. However, systematic investigations on the $8A_u + 7B_u$ infrared-active vibrational
modes of the characteristic monoclinic structure of nanometre $ZrO_2$ have not been reported to
the authors' knowledge. IR spectroscopy has been widely employed in the characterization of
different morphologies of $ZrO_2$ and related materials [5–9], since IR spectra are very sensitive
to local lattice distortions and bond strengths [7, 9]. It has been proposed that [8, 9], due
to their somewhat larger probing depths, the IR spectra may be more sensitive than x-ray

‖ Present address: Physics Department, University of Miami, PO Box 248046, Coral Gables, FL 33124, USA. E-mail
address: hzhang@phyvax.ir.miami.edu.
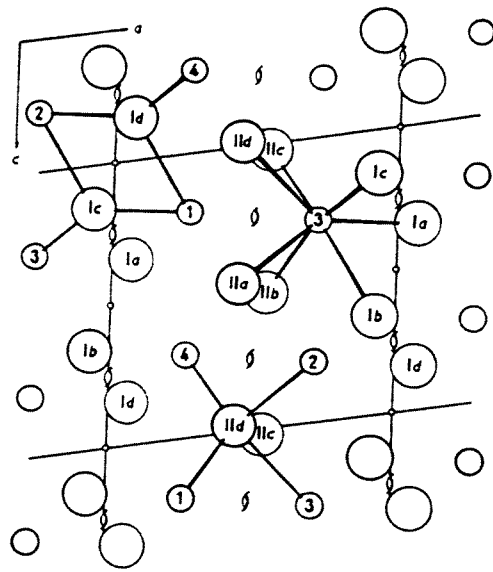
(a)
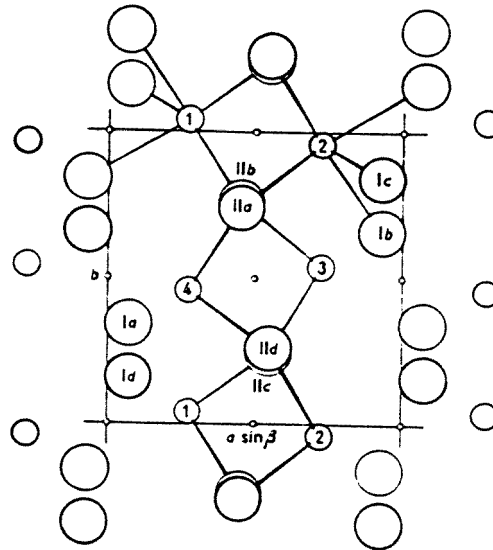


(b)

**Figure 1.** The crystal structure of m-$ZrO_2$: (a) the projection on (010) and (b) the projection on (001); the bigger and smaller circles indicate the O and Zr atoms respectively. (Taken from [11], by permission.)

diffraction (XRD) and Raman spectroscopy in the characterization of the phases and lattice distortions of $ZrO_2$. Moreover, since the IR reflectance measurements can be carried out on as-formed samples without grinding—which may cause some subtle changes in the IR spectra [8]—they are especially favoured for the study of some structures which are susceptible to

mechanical damage. Here we report our measurements on FT-IR spectra of a series of nano-$ZrO_2$ samples with particle sizes ranging from 5 nm to 120 nm. Up to twelve reflectance bands of characteristic m-$ZrO_2$ have been observed, and two surface modes of nanometre grains have been identified. The appearance of more subtle peaks in the spectra of higher-temperature-annealed samples indicates the process of strain removal.

The nano-$ZrO_2$ grains with an average grain diameter of about 5 nm are obtained by a hydrothermal method [3, 10]: the powder was dried in a vacuum desiccator for 14 h and then stored in a desiccator. Nanoclusters having different particle sizes of 10 nm, 15 nm, 90 nm, and 120 nm are obtained by annealing at 300 °C, 500 °C, 900 °C, and 1100 °C, respectively, for eight hours. They are labelled as: n-1 (as-formed), n-2 (300 °C), ..., n-5 (1100 °C) respectively. The samples are pressed into circular discs about 10 mm in diameter and 1.7–1.9 mm in thickness. The average particle diameters have been determined by using TEM micrographs and the XRD method as well [3]. All of the XRD peaks can be attributed to the standard m-$ZrO_2$ structure according to Cohen's method. The FT-IR spectra in the mid-IR region (4000–400 cm$^{-1}$) were recorded on a Bio-Rad FTS 6000 spectrometer with a KBr beam-splitter and a TGS detector; the far-IR spectra were taken by a Bio-Rad FTS 60V spectrometer with a 6.5 $\mu$m Mylar beam-splitter (500–50 cm$^{-1}$) for the reflectance study and a metal wire mesh (700–50 cm$^{-1}$) for the transmission measurement; the resolution is better than 4 cm$^{-1}$. The overlapping ranges of the two spectrometers, i.e., the mid- and far-IR ranges, agree with each other very well. In FT-IR transmission measurements, the samples were dispersed in CsI pellets. In the FT-IR reflectance measurements, a mirror of thin gold film served as the reference; both the sample and the reference measurements were recorded in single-beam form, then their ratio was expressed as the infrared reflectance spectra. All of the spectral measurements were carried out at room temperature.

**Table 1.** The assignments of IR-active modes (in cm$^{-1}$) in m-$ZrO_2$. The temperatures indicated are annealing temperatures, $T_A$. The data from reference [7] and reference [9] are FT-IR reflection results. (Superscript 'sh' stands for shoulder; 's' stands for surface phonon.)

| Reference [2] | | Reference [7] | Reference [9] | Present results | | | | |
|---|---|---|---|---|---|---|---|---|
| | | | | n-5 | n-4 | n-3 | n-2 | n-1 |
| t-$ZrO_2$ | m-$ZrO_2$ | | | 1100 °C | 900 °C | 500 °C | 300 °C | As-formed |
| | 104 A$_u$ | | | | | | | |
| | 180 A$_u$ | | | | | | | |
| | 192 A$_u$ | | | | | | | |
| | 235 A$_u$ | 220 | 222 | 224 | 226 | 226 | 230 | 235 |
| | 270 A$_u$ | 250 | 255 | 257 | 264 | 260 | 260 | 258 |
| | | | | 324$^{sh}$(?) | | | | |
| | 360 B$_u$ | 330 | 320 | 351 | 355 | 349 | 351 | 351 |
| 365 A$_{2u}$ | 375 B$_u$ | 370 | 350 | 376 | 375 | 376$^{sh}$ | 377$^{sh}$s | 373s |
| | 415 A$_u$ | 420 | 420 | 417 | 419 | 415 | 416$^{sh}$ | |
| 435 E$_u$ | 445 A$_u$ | 440 | 445 | 453$^{sh}$ | 445 | | 432s | 434s |
| | 515 2B$_u$ | 520 | 520 | 511 | 503 | 503 | 503 | 505 |
| 575 E$_u$ | 620 2B$_u$ | 600 | 588 | 588 | 588 | 575 | 580 | 580 |
| | | | | 687(?) | 685(?) | 690(?) | | |
| | | | | 725(?) | | | | |
| | 740 A$_u$ + B$_u$ | 740 | | 789 | 779 | 769 | 746 | 738 |

Figure 1 shows the crystal structure of m-$ZrO_2$ with four molecules per unit cell [11]. The group-theoretical analysis gives the zone-centre vibrational modes as $\Gamma = 9A_g + 9B_g + 9A_u + 9B_u$, among which the $9A_g + 9B_g$ are Raman active, and the $8A_u + 7B_u$ are IR active. Figure 2
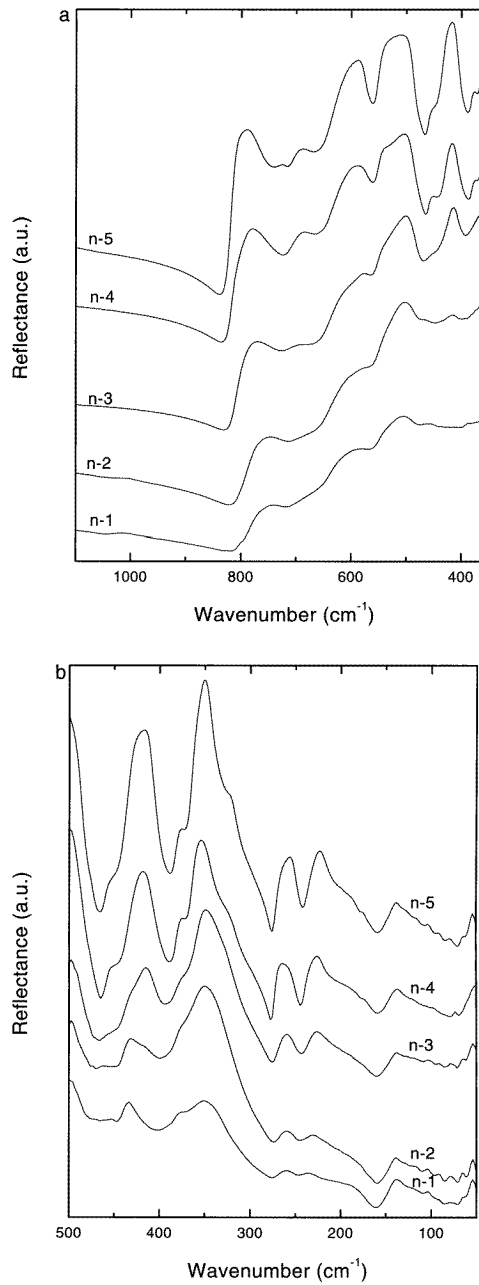
**Figure 2.** The FT-IR reflectance spectra of nanometre $ZrO_2$ with different particle sizes. (a) The mid-IR region; (b) the far-IR region. The corresponding annealing temperatures are indicated in table 1.

and figure 3 show the reflectance and transmission spectra of nano-$ZrO_2$, with (a) and (b) showing their mid- and far-IR regions, respectively. The present high-quality spectra are free of disturbances from $H_2O$ or $CO_2$ in the ambient atmosphere due to the vacuum chambers in FTS
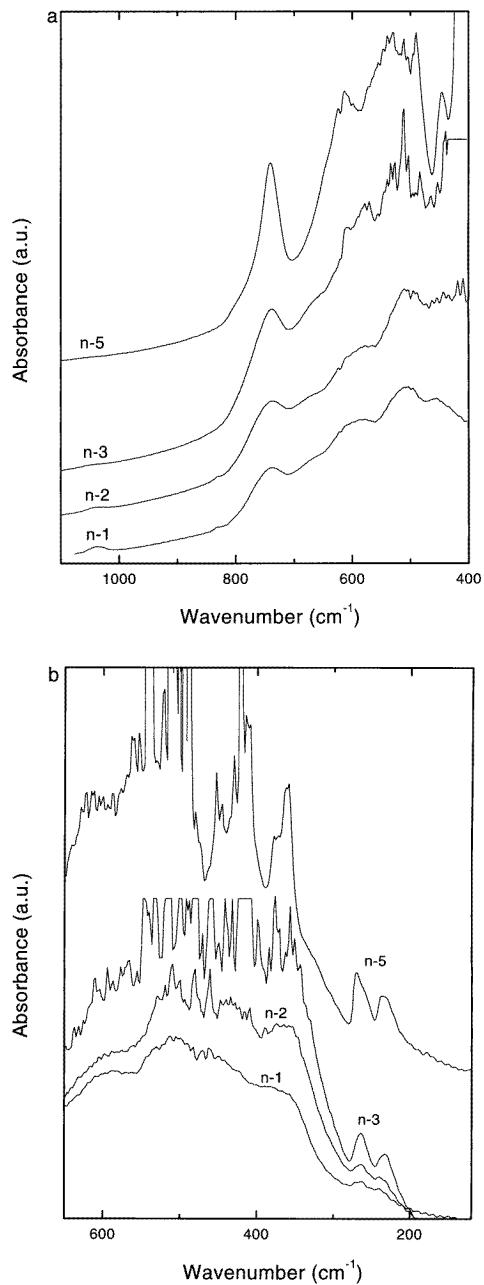
**Figure 3.** The FT-IR transmission spectra of nanometre $ZrO_2$ samples. (a) The mid-IR region; (b) the far-IR region. The corresponding annealing temperatures are indicated in table 1. The n-4 spectrum is not presented since it is even worse than the n-3 spectrum. Part ranges of the n-3 spectrum are cut out for clarity.

60V and the long-time purge of dry gas in the FTS 6000 system. Although the accurate band positions and shapes of the IR reflectance spectra differ slightly from those of the transmission spectra, there is a one-to-one correlation between them; this is the case for many powdered

inorganic materials including $ZrO_2$ [5–9]. Here it should be noted that the samples with higher annealing temperatures $T_A$ (above 500 °C) become less infrared transparent and thus give poor transmission spectra, while the reflectance spectra always have high signal-to-noise ratios and are sharp and therefore more informative [7, 9]. So our discussions will mainly rely on the reflectance spectra. With the help of the transmission spectra and the thoroughly studied reflectance spectra [5–9] of $ZrO_2$, most of the reflectance bands could be assigned clearly.

The n-5 and n-4 samples include all of the standard m-$ZrO_2$ IR-active modes except the three lowest $A_u$ ones, which have not been observed experimentally by previous workers either. The hump at 140 cm$^{-1}$ in the spectra is an anomalous response due to the 6.5 $\mu$m Mylar and thus should not be interpreted as an $A_u$ mode. The results are summarized in table 1. From the spectrum of the n-5 sample, one can see that besides the nine previously observed $5A_u + 7B_u$ bands (table 1), there are three extra bands at 324 cm$^{-1}$, 687 cm$^{-1}$, and 725 cm$^{-1}$. Now, we do not try to re-assign the modes, although the theoretically predicted positions of the three lowest $A_u$ modes may not be accurate [2]. The broad 687 cm$^{-1}$ band is attributed to the combination or overtones of the fundamental vibrational modes. The broad nature of the three bands at 511 cm$^{-1}$, 588 cm$^{-1}$, and 789 cm$^{-1}$ is in accord with the conclusion that they are doubly degenerate [2]. As the particle size decreases, the reflectance bands broaden and begin to merge, making some weak bands invisible. When the particle size decreases to 10 nm (n-2) and 5 nm (n-1), there are eight discrete but broad bands left, which are rooted in a very broad background extending from 300 cm$^{-1}$ to 700 cm$^{-1}$. As the particle size decreases, the surface area increases, and the numbers of atoms and clusters at the surface and interface also increase. As for the previously taken photoacoustic spectra (PAS) of $ZrO_2$ nanoclusters [3], the broadening of the reflectance bands is caused by such a surface effect and the interaction between the nanoclusters. The TEM study shows that nano-$ZrO_2$ particles are nearly spherical but are not well separated; the interactions between the particles and the distribution of the sizes must also account for the broadening of the reflectance bands. As for the broad background, the explanation may be that as the particle sizes decrease, the oxygen vacancies and local lattice distortions gradually appear, lowering the crystal symmetry; thus the relaxation of the selection rules will lead to the appearance of some otherwise optically silent modes in the one-phonon density of states. Previous structural studies [12, 13] on nanometre $SnO_2$ show that the interfaces vary in type from amorphous to polycrystalline; the situations must be similar for nano-$ZrO_2$. An extreme example is provided by the Raman and IR spectra of non-crystalline silicon, in which all vibrational modes become optically active [14].

For such small particle sizes, the spectra should be dominated by both surface excitations and bulk modes [15]. Basically the absorption positions of the surface polar phonon modes can be estimated in terms of the transverse optical modes as [15]

$$\prod_{j=1}^{8} \frac{\omega_{A_u}^{sj}}{\omega_{A_u}^{j}(TO)} = \left( \frac{\varepsilon_{0\parallel} + \varepsilon_m}{\varepsilon_{\infty\parallel} + \varepsilon_m} \right)^{1/2}$$
$$\prod_{j=1}^{7} \frac{\omega_{B_u}^{sj}}{\omega_{B_u}^{j}(TO)} = \left( \frac{\varepsilon_{0\perp} + \varepsilon_m}{\varepsilon_{\infty\perp} + \varepsilon_m} \right)^{1/2} \tag{1}$$

where the $\omega^{sj}$ are frequencies of surface phonons, $\omega^{j}(TO)$ the bulk transverse mode frequencies, $\varepsilon_m$ the dielectric constants of the medium ($\varepsilon_m = 2.62$ for CsI pellets); '$\parallel$' indicates the direction parallel to the $c$-axis and '$\perp$' the perpendicular ones, since the $A_u$ and $B_u$ modes have been identified as the atomic displacements parallel to the $c$-axis and in the $ab$-plane, respectively [7]. However, two difficulties would make such calculations for the present m-$ZrO_2$ unreliable:

(a) excluding the three doubly degenerate $B_u$ modes, there are altogether 12 distinctive group-theoretically predicted IR-active modes—even for bulk materials, at least three $A_u$ modes are missing; for small-particle materials, more modes are missing—thus making the left-hand side of equation (1) uncertain;

(b) most bands appearing for small-grain samples can be assigned to bulk modes, as discussed below.

In fact, six out of the eight bands at 235 cm$^{-1}$, 258 cm$^{-1}$, 351 cm$^{-1}$, 505 cm$^{-1}$, 580 cm$^{-1}$, and 738 cm$^{-1}$ for the n-1 sample could be identified as relating to bulk modes, since their intensities increase as the particle sizes increase—while for typical surface phonons, they would have intensities decreasing with increasing particle sizes [15]. Indeed, the above bands are the characteristic bands of m-$ZrO_2$, as discussed in references [2, 6–9]. In making the identifications of the remaining two bands at 434 cm$^{-1}$ and 373 cm$^{-1}$ (figure 2(b)), however, we should be cautious. On the one hand, the 434 cm$^{-1}$ band weakens as the particle size increases, and almost disappears at $T_A = 500$ °C (n-3). This is just one of the typical characteristics of surface phonons [15]. On the other hand, it also seems to be one of the characteristics of IR-active $E_u$ modes at 435 cm$^{-1}$ in t-$ZrO_2$ (table 1). However, as mentioned at the beginning, t-$ZrO_2$ could be obtained by either heating to about 1425 K or doping with 12 mol% $Y_2O_3$; the possibility of its appearance in as-formed and 300 °C annealed nanometre $ZrO_2$ samples could thus be safely excluded. So the 434 cm$^{-1}$ band is ascribed to surface phonons. So is the 373 cm$^{-1}$ band appearing for the n-1 sample. The interior $B_u$ mode at 376 cm$^{-1}$ is very weak compared with its 'twin' mode at 351 cm$^{-1}$ (as shown for the n-4 and n-5 samples), while the 373 cm$^{-1}$ mode is not so weak compared with the 351 cm$^{-1}$ mode for the n-1 sample. As $T_A$ increases to 500 °C, it almost disappears; at $T_A = 900$ °C and 1100 °C, the 375 cm$^{-1}$ mode should be the interior $B_u$ mode.

Compared with the IR spectra of small-crystal $SiO_2$ [16], ZnSe [17], and MgO [18], which are dominated by surface phonons when their particle sizes reduce to several micrometres, those for $ZrO_2$ nanograins are very unusual in that they retain the main interior IR features even for grain sizes of several nanometres, as demonstrated by the above analysis. This property may find future applications.

The IR spectra of samples n-3 to n-5 also indicate a strain-free process. According to the results of reference [8], the appearance of more subtle spectral bands such as the doublets at around 435 cm$^{-1}$ (453 cm$^{-1}$ and 417 cm$^{-1}$) and 365 cm$^{-1}$ (376 cm$^{-1}$ and 351 cm$^{-1}$) is an indication of a strain-free monoclinic phase (in the n-4 and n-5 spectra), while n-3 ($T_A = 500$ °C) is still a strained sample. The removal of strain from annealing nanograins manifested by IR spectra has also been observed for nanograin $La_{2/3}Ca_{1/3}MnO_3$ [19]. It is well known that the annealing of samples mainly involves three steps: the removal of the internal stress, the interface structure relaxation, and the growth of the grains. Below 800 °C, the removal of the internal stress, the rearrangement of interface atoms and the interface components predominate. Above 800 °C the grains grow quickly with increasing $T_A$. Comparing the spectra of samples n-4 and n-5, one can see that specimen n-5 exhibits more subtle peaks—such as those at 324 cm$^{-1}$ and 725 cm$^{-1}$—than specimen n-4. It can be concluded here that, though not predominant any longer, the process of removing internal stress still continues above 800 °C; at the same time the particle size increases rapidly.

There are two particularly interesting phenomena in the IR reflectance spectra:

(a) the doubly degenerate modes redshift (i.e., shift to lower wavenumber or longer wavelength) as the particle size decreases: the two $B_u$ modes at around 588 cm$^{-1}$ and 511 cm$^{-1}$ shift to 580 cm$^{-1}$ and 505 cm$^{-1}$ respectively; surprisingly, the overlapping $A_u + B_u$ mode at 789 cm$^{-1}$ for sample n-5 shifts to 738 cm$^{-1}$ for sample n-1;

(b) the single modes blueshift (e.g., $A_u$ at 224 cm$^{-1}$ shifts to 235 cm$^{-1}$ in going from sample n-5 to sample n-1), or undergo small displacements (e.g., the $B_u$ mode at 351 cm$^{-1}$). They decrease and broaden as the particle size decreases.

It is also surprising that our IR reflectance frequencies of the overlapping $A_u + B_u$ mode appear at around 790 cm$^{-1}$ for the n-5 sample—i.e., at a very different position to the widely observed one of 740 cm$^{-1}$. The precise reason for this is not known yet. However, it is interesting to note the classification of the internal–external modes according to Anastassakis *et al* [1]: the vibrational modes in m-ZrO$_2$ which are below 450 cm$^{-1}$ are external modes which describe the ZrO$_2$ 'molecules' vibrating as rigid units, while those above 450 cm$^{-1}$ are internal modes in which the Zr or O atoms vibrate relative to each other. Here the three doubly degenerate modes are above 450 cm$^{-1}$; thus they are internal vibrations. As the particle sizes decrease, the increasing of surface components, local lattice distortions, and dangling bonds may soften the relative displacements of Zr and O atoms (internal modes) to some extent, while they may have less effect on the translation and libration movements of the molecules (external modes). This tentative argument should be subjected to further investigations.

In conclusion, we have obtained high-quality FT-IR reflectance spectra of nanometre ZrO$_2$ with particle sizes ranging from 5 nm to 120 nm. The fact that six characteristic m-ZrO$_2$ reflectance bands and only two surface bands appear for very small grains (5–10 nm) shows that the nanograins remain the main symmetry features of m-ZrO$_2$. The removal of internal stress persists to higher annealing temperatures. The annealing of nanometre ZrO$_2$ has different effects on the doubly degenerate and the single IR-active modes.

## Acknowledgments

## References

[1]  Anastassakis E, Papanicolaou B and Asher I M 1975 *J. Phys. Chem. Solids* **36** 667
[2]  Feinberg A and Perry C H 1981 *J. Phys. Chem. Solids* **42** 513
[3]  Xiong Y H, Yu K N and Xiong C S 1994 *Phys. Rev.* B **49** 5607
     Xiong Y H, Yu K N and Xiong C S 1994 *Phys. Rev.* B **50** 11 287
[4]  Liu F, Yang J and Zhao T 1997 *Phys. Rev.* B **55** 8847
[5]  Liu D W, Perry C H and Ingel R P 1988 *J. Appl. Phys.* **64** 1413
[6]  Perry C H, Lu F, Liu D W and Alzyab B 1990 *J. Raman Spectrosc.* **21** 577
[7]  Hirata T 1994 *Phys. Rev.* B **50** 2874
[8]  Phillippi C M and Mazdiyasni K S 1971 *J. Am. Ceram. Soc.* **54** 254
[9]  Hirata T, Asari E and Kitajima M 1994 *J. Solid State Chem.* **110** 201
[10]  Morgan P E D 1984 *Commun. Am. Ceram. Soc.* **67** C204
[11]  McCullough J D and Trueblood K N 1959 *Acta Crystallogr.* **12** 507
[12]  Wang D, Wen S, Chen J, Zhang S and Li F 1994 *Phys. Rev.* B **49** 14 282
[13]  Yu K N, Xiong Y, Liu Y and Xiong C 1997 *Phys. Rev.* B **55** 2666
[14]  Brodsky M H and Cardona M 1978 *J. Non-Cryst. Solids* **31** 81
[15]  Ruppin R 1982 *Electromagnetic Surface Modes* ed A D Boardman (New York: Wiley) ch 2 and references therein
[16]  Steyer T R, Day K L and Huffman D R 1974 *Appl. Opt.* **13** 1586
[17]  Genzel L and Martin T P 1973 *Surf. Sci.* **34** 33
[18]  Srivastava S P and Singh R D 1971 *Chem. Phys. Lett.* **10** 387
[19]  Li K, Cheng R, Wang S and Zhang Y 1998 *J. Phys.: Condens. Matter* **10** 4315